Progress In Electromagnetics Research M, Vol. 72, 105–114, 2018

Design and Development of a Novel EBG Cell

Sukhdas Ahirwar[1, *], Dasari Ramakrishna[2], and Vijay M. Pandharipande[2]

Abstract—In this paper, design and development of a novel electromagnetic band gap cell is presented. The EBG cell is designed aiming its use at relatively low frequencies. It is designed as a uni-planar structure to simplify the fabrication process. It consists of multiple parallel combinations of L and C. These components are realized using planar microwave integrated circuit technology. The components L & C are designed as a meander-line inductor and inter-digital capacitors, respectively. The cell is perfectly symmetrical along x and y-axes to have uniform performance along two orthogonal directions. It is evaluated for its S-parameters and reflection phase. Simulated and measured results are presented for frequency range of 0.885 GHz to 3.1 GHz.

1. INTRODUCTION

Electromagnetic band-gap (EBG) structures are artificially engineered materials providing the electromagnetic properties which are not available in natural materials. Electromagnetic band gap (EBG) structures are also known as photonic band gap (PBG), high impedance surface (HIS), metamaterial (MTMs) or electromagnetic crystals (ECs). These materials exhibit a frequency band gap across which electromagnetic wave cannot propagate. The electromagnetic band gap structures are the periodic structures with cell size much smaller than the free space wave length [1]. The property of EBG material to suppress the propagation of surface wave in a particular frequency band is exploited for various applications by embedding the EBG structure with ground plane. The EBG structure consisting of EBG cells in a periodic manner can be used

(1) in antenna technology to enhance antenna gain and reduce back lobe radiation [2, 3], to reduce mutual coupling between antenna elements [4–6] and to improve impedance matching [7–9];
(2) in printed circuit boards to reduce the noise in the circuits;
(3) in packaging technology [10];
(4) in microwave devices where these devices can be tuned using EBG structure [11] and
(5) in microwave filter design [12].

A very basic EBG structure consisting of metal patches on the grounded substrate with vertical vias is known as mushroom-like surface [13]. A similar arrangement without vertical vias is also reported [14, 15] and is called as a uni-planar structure design. The mushroom-like EBG surface has a lower frequency of operation and smaller size than uni-planar EBG surface. The uni-planar EBG surface is advantageous over mushroom-like EBG surface in terms of performance sensitivity to the incident angle and polarization [16]. A uni-planar EBG structure consisting of simple square patches on a grounded substrate is modified to achieve a Uni-planar Compact Photonic Bandgap (UC-PBG) structure. In UC-PBG structure design, the patches or modified patches are inter-connected with sections of microstrip lines. These lines provide the required inductance to form an LC circuit.

Received 18 April 2018, Accepted 1 August 2018, Scheduled 21 August 2018
* Corresponding author: Sukhdas Ahirwar (sdahirwar@rediffmail.com).
[1] Defence Electronics Research Laboratory (DLRL), Hyderabad 500005, India. [2] Centre for Excellence in Microwave Engineering (CEME), Department of ECE, University College of Engineering, Osmania University, Hyderabad 500007, India.

In this paper, L and C values are designed on the same surface of a grounded substrate. The higher values of L and C along with circuit compactness are achieved by meander-line inductor and inter-digital capacitor designs, respectively. The higher values of L and C insure lower resonance frequency of Parallel LC tuned circuit.

2. EBG CELL DESIGN

Considering any electromagnetic wave travelling along any general impedance surface, the properties of TM and TE surface waves can be described with single parameter called surface impedance (Z_s) [17, 18]. This impedance is given by

$$Z_s(TM) = j\alpha/\omega\varepsilon \tag{1}$$

$$Z_s(TE) = -j\omega\mu/\alpha \tag{2}$$

Equations (1) and (2) show that the TM waves are supported by a surface having positive reactance (inductive surface), and TE waves are supported by the surface having negative reactance (capacitive surface). The impedance and resonance frequency of parallel LC circuit is given by the following equations —

$$Z = j\omega L/\left(1-\omega^2 LC\right) \tag{3}$$

$$f_0 = 1/(2\pi\sqrt{LC}) \tag{4}$$

At lower frequencies the circuit impedance is positive, and the surface supports the TM waves. At higher frequencies the impedance is negative supporting the TE waves. At resonance frequency, the EBG structure provides high impedance to the surface waves, and the electromagnetic band gap for a particular frequency band is observed.

In the proposed design, the parallel LC circuit is realized by printed inter-digital capacitors and meander-line inductors on a grounded 3 mm thick FR4 substrate having $\varepsilon_r = 4.4$. In the form of 2D surface, four pairs of LC circuits are used to form the EBG cell. The symmetry of the EBG cell is very important to have the uniform performance in both x- and y-directions. This cell is modelled in ADS circuit simulator software. Circuit schematic for full cell and one-fourth part of it for better clarity are shown in Figs. 1(a) and 1(b), respectively. Each section of the parallel LC circuit is rotated by 90° cyclically from previous one to have perfect symmetry in two orthogonal directions. Layout of the circuit and its equivalent circuits are shown in Figs. 2(a) and 2(b), respectively. The cell is designed to have its frequency band of operation at lower frequencies (1 GHz or less) as most of EBG cell structures are not suitable at lower frequencies due to size constraints. The overall size the cell is restricted to 50 mm × 50 mm. Electrically this size is 0.15λ at lower frequency of operation. The dimensional details of meander-line inductor and inter-digital capacitor are shown in Table 1.

Table 1. Dimensional parameters of inter-digital capacitor and Meander-line inductor.

Inter digital capacitor							Meander line Inductor			
W_f (mm)	W_t (mm)	W (mm)	G (mm)	G_e (mm)	L (mm)	N	W (mm)	S_1 (mm)	S_2 (mm)	N
2	2	2	1	1	21	4	2	1	4	4

3. RESULTS AND DISCUSSIONS

3.1. Measurement of Surface Wave Suppression Characteristics

The surface waves exist at the conductor-dielectric interface due to different electrical properties of the medium. One practical example of this is a patch antenna. In this antenna, surface waves exist between ground plane and radiating element. Some power is wasted in the form of surface wave which does not contribute in radiation. It is shown [19] that $\varepsilon^{3/2}$ times the available power is wasted due to surface

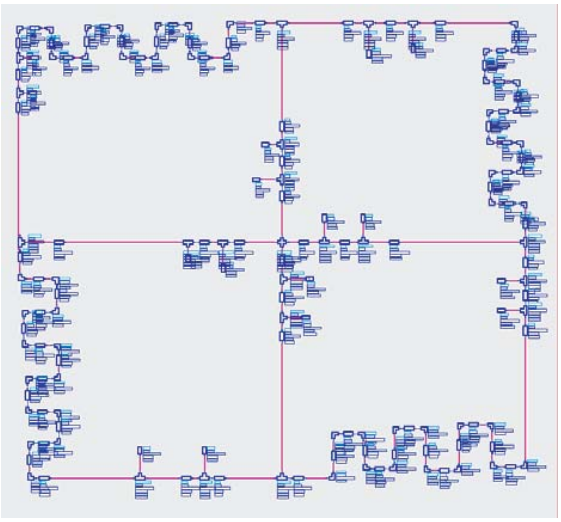

(a)

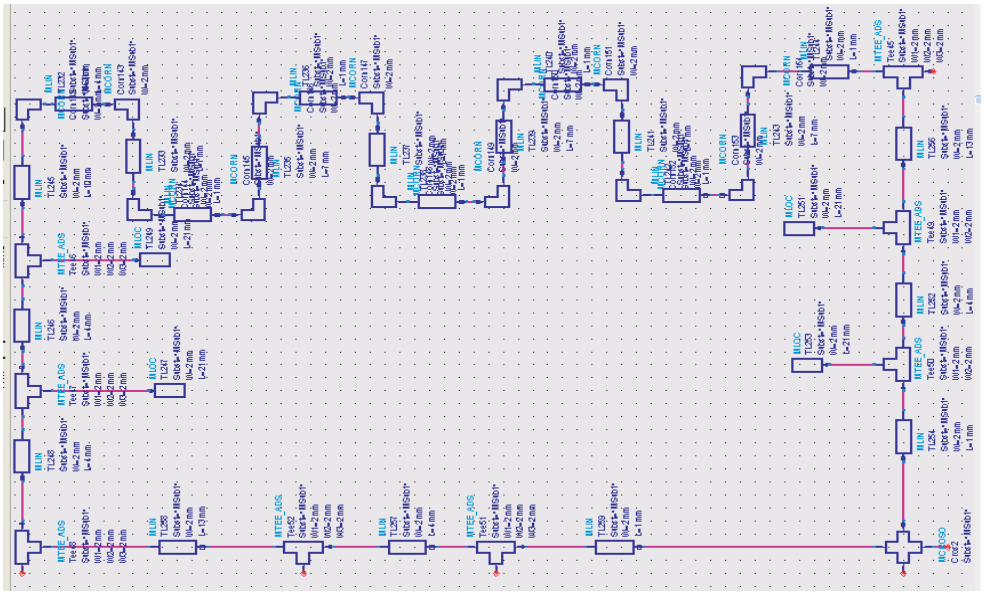

(b)

Figure 1. (a) Schematic of proposed EBG cell. (b) Schematic of one-fourth part of proposed EBG cell.

wave, and the antenna efficiency is decreased accordingly. When the surface has more impedance than the impedance of the medium from which the wave is impinging on the surface, the wave reflects from the surface, and transmission through this surface is minimised.

The reflection coefficient is expressed in terms of impedances of two media and angle of incident as follows [20] —

$$\Gamma = (Z_s \cos\theta - \eta_0)/(Z_s \cos\theta + \eta_0) \tag{5}$$

where Z_s is the surface impedance, θ the angle of incidence, and η_0 the impedance of free space. For larger value of Z_s the reflection is more and less transmission of the signal through the surface. The reflected and transmitted powers through the surface are measured in terms of S-parameters. S_{11} and S_{21} are the measure of reflected and transmitted powers.

The resonance behaviour of the proposed EBG cell is primarily investigated with ADS circuit simulator with ports attached at two sides. The EBG cell is connected between two ports with 50 Ω port termination. A 50 Ω microstrip line is used to connect the cell to ports. It is simulated in the

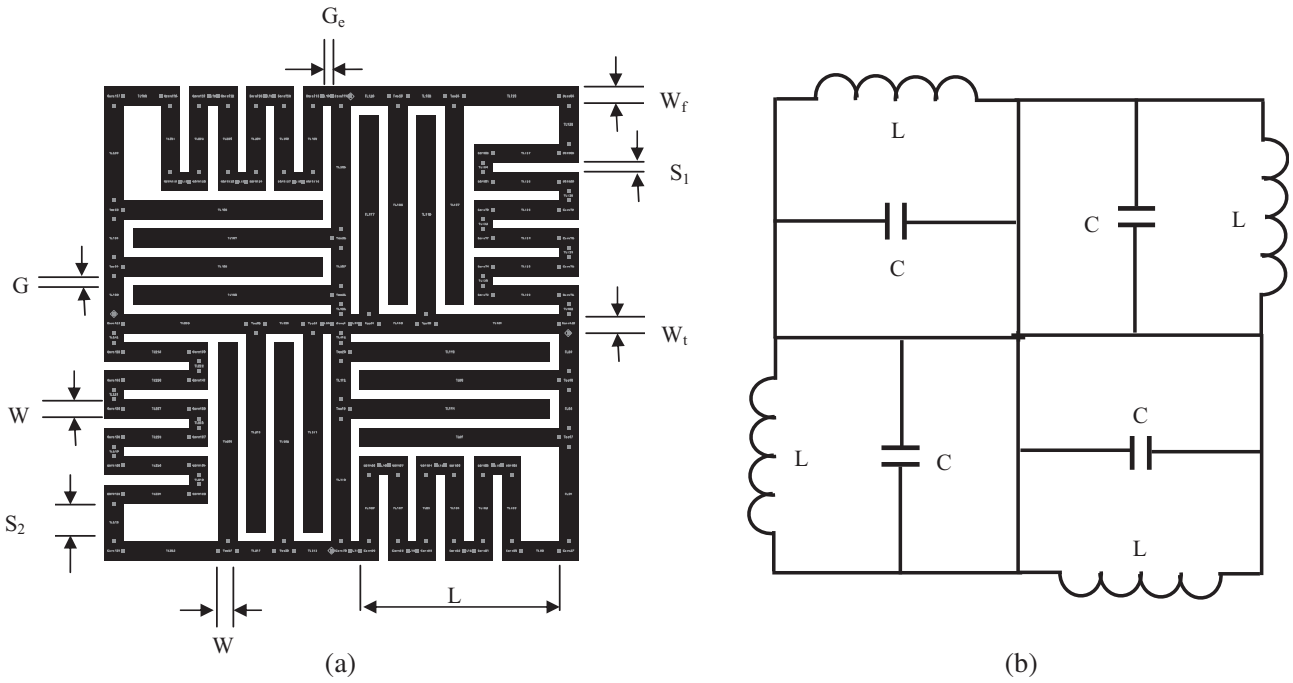

Figure 2. (a) Layout of proposed EBG cell. (b) Equivalent circuit of proposed EBG.

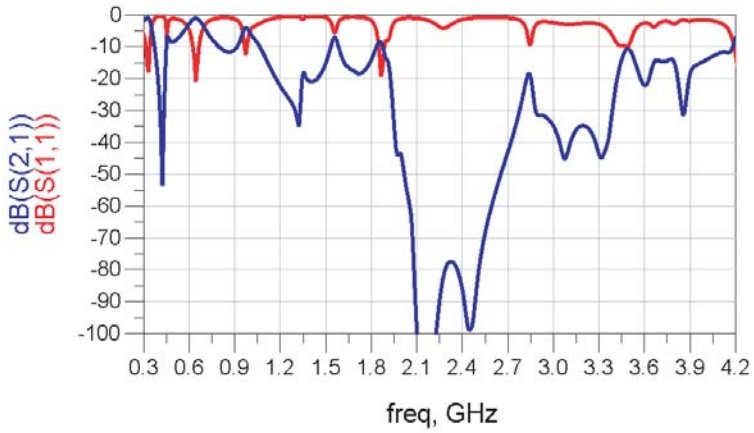

Figure 3. Simulated S-parameters of proposed EBG cell.

frequency range of 0.3 GHz to 4.5 GHz. Simulated S-parameters are shown in Fig. 3. The first resonance is observed at 0.420 GHz. The 10 dB bandwidth for S_{21} is observed in the frequency range of 0.370–0.445 GHz. A continuous stopband is observed from 1.070 GHz to 4.2 GHz with small peaks in S_{21} at 1.560 GHz and 1.860 GHz.

This cell is also studied for different parameters such as strip width and gap between the strips, number of turns of the meander-line inductor and number of fingers of inter-digital capacitor. The parametric values for two cases are tabulated in Table 2.

The overlay of simulated transmission coefficient plots for all three cases is shown in Fig. 4. It is observed from this study that by increasing the number of turns in inductor and number of fingers in capacitor, the values of L and C increase respectively, and lower frequency response is improved. However, at higher frequencies peaks in S_{21} are more pronounced, and the cell behaves as a dual-band structure instead of a broadband structure.

Table 2. Dimensional parametric study in inter-digital capacitor and Meander-line inductor.

	Inter-digital capacitor	Meander-line Inductor
Case-1	Same as in Table 1	$W = 1$, $S_1 = S_2 = 0.5$, $N = 9$
Case-2	$W_f = W_t = W = 1$, $G = G_e = 0.5$ and $N = 9$	Same as in Case-1

In order to reverify these results the structure is modelled with an FDTD based EM simulation tool. The performance evaluation of the EBG cell is carried out with simulation software with simulation set up as suggested in [21]. This simulation model is shown in Fig. 5. In this model, EBG cell is connected between two 50 Ω microstrip lines, and performance is evaluated by the method used to evaluate the microwave filter. This method is also known as directive transmission method [22]. Simulated S-parameters of this model are shown in Fig. 6. As evident from this result, the transmission coefficient S_{21} is similar to that obtained with ADS simulation software, but in this case the low band resonance is

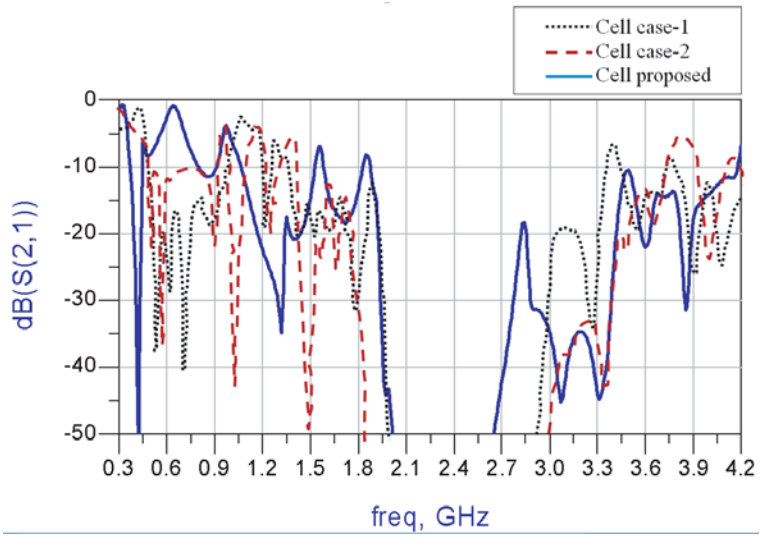

Figure 4. Parametric study of proposed EBG cell for S_{21}.

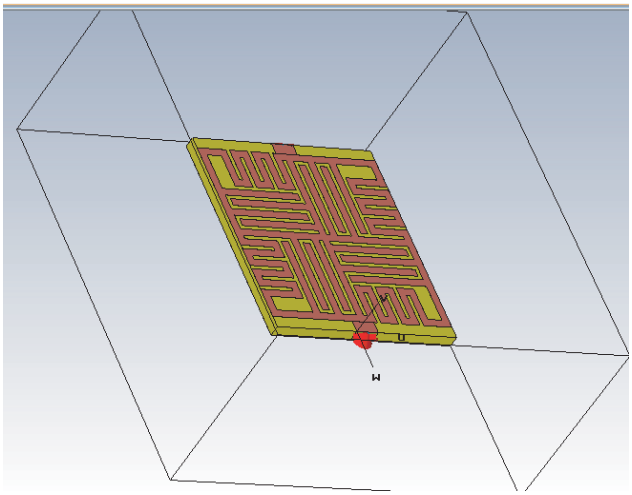

Figure 5. Simulation model of proposed EBG cell.

absent, and the lower frequency of operation is shifted to 0.885 GHz. Similarly, at higher band edge the operating frequency is reduced to 3.1 GHz from 4.2 GHz. Also in this frequency band, the value of S_{21} is slightly less than 10 dB at certain frequency pockets. This is supposed to be the actual frequency band of operation because in the circuit simulation software the reflection and radiation losses may not be considered. In characterization of the EBG structures, value of S_{11} is also equally important. In most of the publications, this parameter is ignored. Drop in S_{21} may be due to reflection, signal attenuation loss and radiation loss. For EBG structure, this drop in S_{21} should be contributed mainly by reflection loss. For high impedance surface (HIS), the impedance mismatch is more between the two media, and signal reflection will be more. Accordingly, the return loss (value of S_{11}) must be lower for larger drop (more insertion loss) in value of S_{21}. This trend of S-parameters can be seen clearly in Fig. 6. This performance of the proposed EBG cell is compared with performances of the mushroom-like [14] and uni-planar structure [15] EBG cells. For this, these cells are modelled with FDTD based EM simulation tool, and cell size is chosen similar to the proposed EBG cell for one-to-one comparison. Comparison

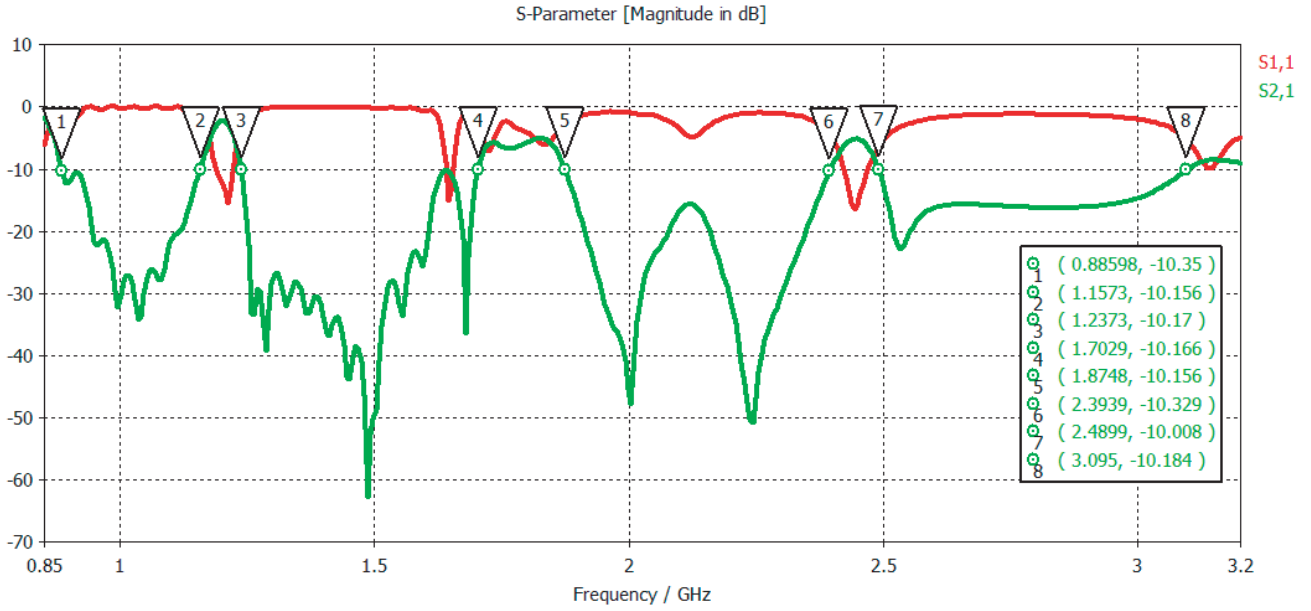

Figure 6. Simulated S_{11} and S_{21} parameters of proposed EBG cell.

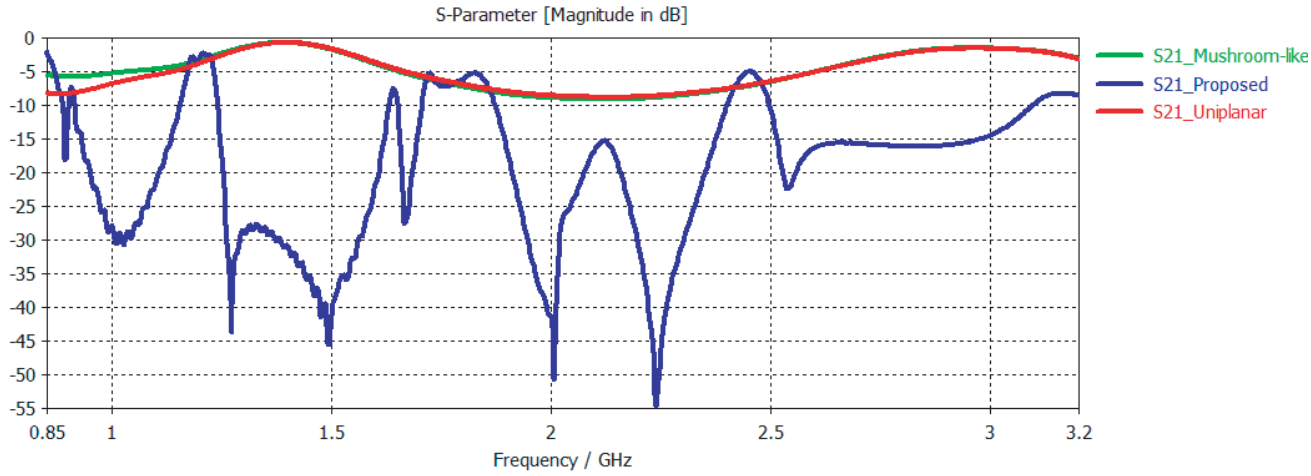

Figure 7. Performance comparison of proposed EBG Cell with conventional EBG cells.

of transmission loss (S_{21}) for these EBG cells is shown in Fig. 7. As can be observed from the overlay of the results, value of S_{21} for mushroom-like and uni-planar is much lesser than the proposed EBG cell. A single cell as shown in the model is fabricated using printed circuit technology. A photograph of this cell is shown in Fig. 8. This EBG cell is evaluated for its S-parameters using M/s Agilent E5071C Vector network Analyser. The overlaid plot of simulated and measured S_{21} parameters for the proposed EBG cell is shown in Fig. 9. The measured results are in good agreement with simulated parameters. In measured results, the small peaks in S_{21} at certain frequency pockets disappear, and an improvement in measured S_{21} is observed. This may be attributed to the test conditions in simulation and practical measurement. In simulation, ideal conditions are assumed which are not possible in actual measurement.

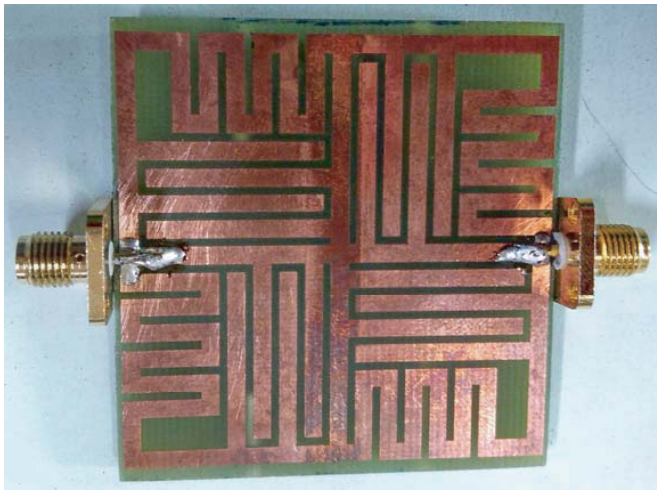

Figure 8. Photograph of the proposed EBG cell.

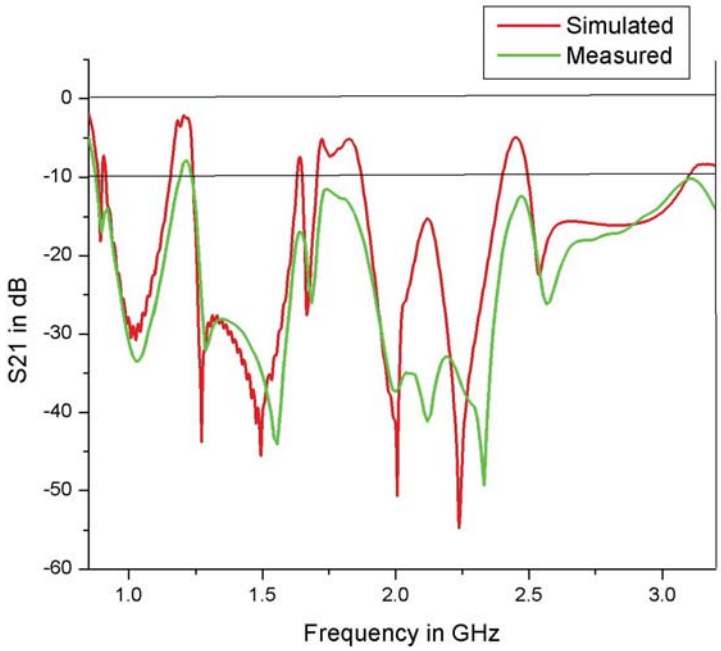

Figure 9. Simulated and measured S_{21} of the proposed EBG cell.

3.2. Measurement of Reflection Phase Characteristics

The behaviour of a wave changes as it travels from one medium to another medium. This behavioural change is dependent on the electrical parameters of medium. If one medium has its electrical parameters as σ_1, μ_1 and ε_1 and the corresponding parameters for other media are σ_2, μ_2 and ε_2, then reflection, refraction and transmission characteristics of the wave change from one medium to other. When a wave travels from one medium to other, it may be partially/fully transmitted in another medium or partially/fully reflected in the same medium. The phase of reflected wave is dependent on the medium parameters mentioned above. For perfect electrical conductors (PEC), the phase of reflected wave is ± 180 deg. with respect to incident wave, and the surface behaves as a short circuit for the wave. For high impedance surface, the phase of the reflected wave is 0 deg. with respect to incident wave, and this surface behaves as artificial magnetic conductor (AMC). Since the working principle of an EBG structure also involves high impedance characteristics of the structure, the performance of the EBG structure can also be evaluated by reflection phase of the wave encountering such type of the structure.

Reflection phase of a wave for any surface is calculated with reference to PEC surface having reflection phase of ± 180 deg. For calculation of the reflection phase, wave is launched to the surface from a point near the surface, and the phase of the reflected wave is measured. At the observation point, the phase is related to different phase components as per relation [22] given below —

$$\theta_\Gamma = \theta_{\Gamma(S)} + \theta_{\Gamma(PEC)} - 180 \text{ deg.} \tag{6}$$

where θ_Γ = total reflection phase at the point of observation, $\theta_{\Gamma(S)}$ = reflection phase at the surface and $\theta_{\Gamma(PEC)}$ = reflection phase of PEC.

Using above equation the reflection phase of the surface ($\theta_{\Gamma(S)}$) can be calculated. It is shown [11] that bandwidth of an EBG structure is given by

$$BW = Z_0/\eta_0 \tag{7}$$

where $Z_0 = \sqrt{L/C}$ is the characteristics impedance of LC circuit, and η_0 is the impedance of free space. For the operational bandwidth of EBG given by above equation, the range of reflection phase is $-90°$ to $+90°$. If the reflection phase lies in this range, the structure can be approximated as AMC. In low profile antenna applications it is also reported [23] that this reflection phase can also be considered as satisfactory in the range of $90° \pm 45°$.

For simulation of the reflection phase, the port is created at the point of observation, and the structure is simulated with appropriate boundary conditions.

The proposed EBG cell is modelled in an FDTD based simulation software. This simulation model is shown in Fig. 10. After assigning proper boundary conditions (PEC and PMC) and excitation port

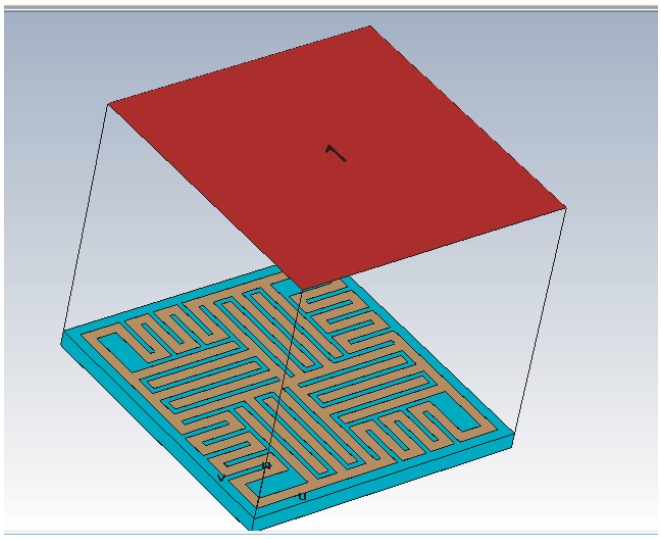

Figure 10. Simulation model of the proposed EBG cell.

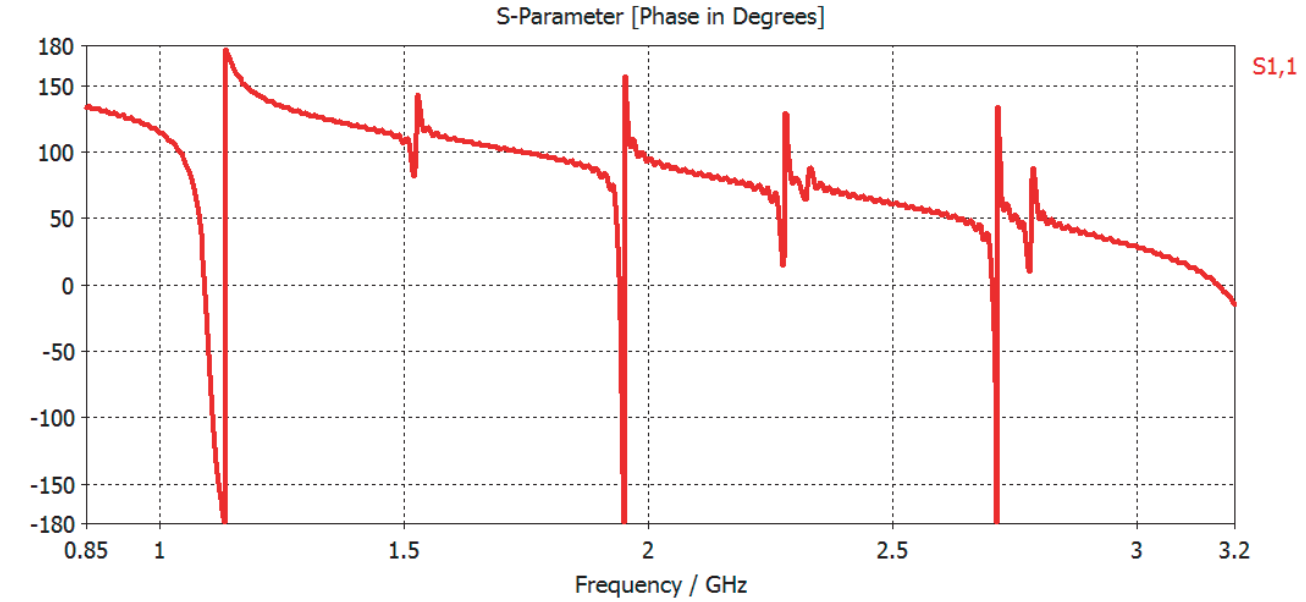

Figure 11. Simulated reflection phase of proposed EBG Cell.

(wave guide port), the structure is simulated for phase of reflected wave. Simulated reflection phase is shown in Fig. 11. As evident from the result, the reflection phase is well within the limit for the structure to have the properties of AMC.

4. CONCLUSION

A new type of EBG cell has been designed and developed. The L and C components are realised in the form of meander-line inductor and inter-digital capacitor, respectively. For realisation of inductance, via is avoided, and hence structure fabrication is less costly and simple. The structure is uni-planar and can be fabricated easily using printed circuit technology. Performance of this cell is evaluated by evaluation of its S-parameters and reflection phase. These parameters are simulated using the simulation tools. The achieved results are validated by measurement. The achieved bandwidth is more than $3:1$. Being symmetrical in both x- and y-directions, the performance of this 2D structure is independent of the two orthogonal directions. The EBG cell can be configured as periodic structure or as inter connected cells. Depending upon the requirements, the structure can be integrated in the form of EBG ground plane.

ACKNOWLEDGMENT

Authors would like to sincerely thank Dr. A. K. Singh, OS and Director, DLRL and Shri M. Balachary, OS & Associate Director, DLRL, for constant encouragement and support for carrying out the research work.

REFERENCES

1. Mahmoud, S. F., "A new miniaturized annular ring patch resonator partially loaded by a meta material ring with negative permeability and permittivity," *IEEE Antennas and Wireless Propagation Letters*, Vol. 3, No. 1, 19–22, 2004.
2. Gonzalo, R., P. de Maagt, and M. Sorolla, "Enhanced patch-antenna performance by suppressing surface waves using photonic-bandgap substrates," *IEEE Trans. Microw. Theory Tech.*, Vol. 47, No. 11, 2131–2138, Nov. 1999.

3. Yang, F. and Y. Rahmat-Samii, *Electromagnetic Band Gap Structures in Antenna Engineering*, Cambridge University Press, 2009.
4. Yang, F. and Y. Rahmat-Samii, "Mutual coupling reduction of microstrip antennas using electromagnetic band-gap structure," *Proc. IEEE AP-S Int. Symp. Dig.*, Vol. 2, 478–481, Jul. 2001.
5. Yang, F. and Y. Rahmat-Samii, "Microstrip antennas integrated with electromagnetic band-gap (EBG) structures: A low mutual coupling design for array applications," *IEEE Trans. Antennas Propag.*, Vol. 51, No. 10, 2939–2949, Oct. 2003.
6. Alam, M. S., M. T. Islam, and N. Misran, "A novel compact split ring slotted electromagnetic band gap structure for micro strip patch antenna performance enhancement," *Progress In Electromagnetic Research*, Vol. 130, 389–409, 2012.
7. Yang, F. and Y. Rahmat-Samii, "Reflection phase characterizations of the EBG ground plane for low profile wire antenna applications," *IEEE Trans. Antennas Propag.*, Vol. 51, No. 10, 2691–2703, Oct. 2003.
8. Abedin, M. F., M. Z. Azad, and M. Ali, "Wideband smaller unit-cell planar EBG structures and their application," *IEEE Trans. Antennas Propag.*, Vol. 56, No. 3, 903–908, Mar. 2008.
9. Xu, H.-J., Y.-H. Zhang, and Y. Fan, "Analysis of the connection section between K connector and microstrip with Electromagnetic Band gap (EBG) structure," *Progress In Electromagnetics Research*, Vol. 73, 239–247, 2007.
10. Kim, M. and D. G. Kam, "Wideband and compact EBG structure with balanced slots," *IEEE Transactions on Components, Packaging and Manufacturing Technology*, Vol. 5, No. 6, 818–827, Jun.2015.
11. Karim, M. F., A. Q. Li, A. Yu, and A. Alphone, "Tunable filter using fractal Electromagnetic Band Gap (EBG) structures," *Sensors and Actuators A*, Vol. 133, No. 2, 355–362, 2007.
12. Gao, M.-J., L.-S. Wu, and J. F. Mao, "Compact notched ultra-wideband bandpass filter with improved out-of-band performance using quasi electromagnetic band gap structure," *Progress In Electromagnetics Research*, Vol. 125, 137–150, 2012.
13. Sievenpiper, D., L. Zhang, R. F. J. Broas, N. G. Alexopolus, and E. Yablonovitch, "High-impedance electromagnetic surfaces with a forbidden frequency band," *IEEE Trans. Microw. Theory Tech.*, Vol. 47, No. 11, 2059–2074, 1999.
14. Yang, F.-R., K.-P. Ma, Y. Qian, and T. Itoh, "A Uniplanar Compact Photonic Bandgap (UC-PBG) structure and its applications for microwave circuits," *IEEE Trans. Microw. Theory Tech.*, Vol. 47, No. 8, 1509–1514, 1999.
15. Lin, B.-Q., Q.-R. Zheng, and N.-C. Yuan, "A novel planar PBG structure for size reduction," *IEEE Microwave and Wireless Components Letters*, Vol. 16, No. 5, 269–271, May 2006.
16. Yang, F. and Y. Rahmat-Samii, *Electromagnetic Band Gap Structures in Antenna Engineering*, ISBN-13 (e-book), Cambridge University Press, 2009.
17. Collin, R., *Field Theory of Guided Waves*, 2nd Edition, IEEE Press, New York, 1991.
18. Kovács, P. and T. Urbanec, "Electromagnetic Band Gap structures: Practical tips and advice for antenna engineers," *Radioengineering*, Vol. 21, No. 1, Apr. 2012.
19. Brown, E. R., C. D. Parker, and E. Yablonovitch, "Radiation properties of a planar antenna on a photonic-crystal substrate," *J. Opt. Soc. Am. B*, Vol. 10, No. 2, 404–407, 1993.
20. Simovski, C. R., P. Maagt, and I. V. Melchakova, "High impedance surfaces having resonance with respect to polarization and incident angle," *IEEE Trans. Antennas Propag.*, Vol. 53, No. 3, 908–914, 2005.
21. Lin, B.-Q., Q.-R. Zheng, and N.-C. Yuan, "A novel planar PBG structure for size reduction," *IEEE Microwave and Wireless Components Letters*, Vol. 16, No. 5, 269–271, May 2006.
22. Alam, M. S. and M. T. Islam, "Design of a wideband compact Electromagnetic Band Gap structure for lower frequency applications," *Przegląd Elektrotechniczny*, ISSN 0033-2097, R. 89 NR 4/2013.
23. Yang, F. and Y. Rahmat-Samii, "Reflection phase characterizations of the EBG ground plane for low profile wire antenna applications," *IEEE Trans. Antennas Propag.*, Vol. 51, No. 10, 2691–2703, 2003.